# Input-Output Feedback Linearization Control for a PWR Nuclear Power Plant

Amine Naimi[1], Jiamei Deng[1,*], Akbar Sheikh-Akbari[1], S. R. Shimjith[2] and A. John Arul [3]

***Abstract*— This study proposes a feedback linearization-based control using a dynamic neural network to control a pressurized water-type nuclear power plant. The nonlinear plant model adopted in this study is characterized by five inputs, five outputs and, 38 state variables. The model is linearized through dynamic neural network-based system identification and feedback linearization. The proportional–integral–derivative (PID) controller is subsequently applied to the linearized process. The effectiveness of the proposed approach is demonstrated by simulations on different subsystems of a pressurized water reactor nuclear power plant model. Simulation results show that the proposed strategy offers good performance and is capable of effectively tracking the reference under disturbances.**

## I. Introduction

Nuclear power plants (NPPs) have the characteristic of being complex and highly nonlinear. Moreover, they are subject to parameter variations mainly caused by internal reactivity feedback, fuel burn-up, and modelling uncertainties. NPP operation and control pose a significant challenge, especially when the load-following mode of operation is desired. In fact, daily load cycles can significantly affect the performance of a plant because of the wide range of power variations. Therefore, it is of greatest importance to design an appropriate controller to ensure that the NPP power tracks the power set-point, while ensuring the safety and good operability of the process.

Proportional–integral–derivative (PID) controllers have been designed for the load-following operation of nuclear reactors [1]–[3]. The PID controller performance depends on the gain values used; hence, to achieve better performance, it is important that the PID gains are tuned in an optimal manner. In recent works, intelligent algorithms have been used for the gain tuning of PID controllers [4], [5]. Linear robust controllers have also been employed for the temperature and power control of NPPs. *Banavar et al.* [6] proposed an $H_\infty$ control based on normalized co-prime factorization approach for the power-level control of a pressurized heavy-water reactor (PHWR). *Yan et al.* [7] designed an $H_\infty$ controller to attain stability in power operations in the presence of external disturbances and model uncertainties for a small pressurized water reactor (PWR). Further, the technique of linear quadratic control with loop transfer recovery has been employed to enhance robustness and deal with parameter uncertainties in a load-following PWR [8], [9]. Nevertheless, the performance of these robust controllers is valid only in a limited range because they are based on linear models. Hence, it is essential to design control strategies capable of performing in a wide range of operations, such as the load-following mode.

Nonlinear control approaches such as backstepping (BST), sliding mode control (SMC) and feedback linearization (FBL) have been proposed to overcome these issues. *Wei et al.* [10] used a BST control for the water level regulation of a nuclear U-tube steam generator. *Dong et al.* [11] proposed an approach based on BST and feedback dissipation to control the power level of a nuclear reactor. *Ansarifar et al.* [12] employed an SMC strategy to control a PWR in load-following operation, ensuring that the xenon chattering was maintained within acceptable limits. In a more recent study [13], the SMC was combined with the conventional FBL; performance was improved and the chattering effect was significantly reduced. *Liu et al.* [14] also applied the FBL technique with linear active disturbance rejection (LADR) for a PWR. The main disadvantage of these controllers is that they require an exact mathematical model of the PWR system.

Neural networks (NNs) have an inherent ability to learn and approximate nonlinear systems with an arbitrary accuracy [15]. Some kinds of feedforward NNs provided suitable and improved modeling performance in PWR systems [16]–[18]. However, the main drawback of feedforward NNs is that they are essentially static and limited in representing complex systems. Conversely, dynamic neural networks (DNNs) have proved to be more effective than static NNs due to their structures [19]. The simplicity of their architectures makes them suitable together with nonlinear control techniques [21]–[24]. This paper proposes a DNN-based FBL approach for the effective control of an entire PWR. The DNN is trained to approximate the dynamic behavior of the nonlinear process, and it is used to compute the FBL control law. The effectiveness of the proposed strategy was validated on the five loops of the PWR system, namely the reactor core, steam generator, pressurizer pressure and level, and the turbine speed loops. The proposed control scheme was tested under external disturbances and compared with the performance of the classical model predictive controller.

*Corresponding author.

[1]Amine Naimi (amine.naimi01@gmail.com), Jiamei Deng (j.deng@leedsbeckett.ac.uk) and Akbar Sheikh-Akbari (a.sheikh-akbari@leedsbeckett.ac.uk) are affiliated with the School of Built Environment, Engineering, and Computing, Leeds Beckett University, Leeds, England.

[2]S. R. Shimjith (srshim@barc.gov.in) is with Reactor Control Division, Bhabha Atomic Research Centre, Mumbai, India and Professor, Homi Bhabha National Institute, Mumbai, India.

[3]A. John Arul (arul@igcar.gov.in) is with Probabilistic Safety, Reactor Shielding and Nuclear Data Division, Indira Gandhi Centre for Atomic Research, Kalpakkam, India and Professor, Homi Bhabha National Institute, Mumbai, India.

It was demonstrated that the controller can effectively handle the disturbances and track the desired set point demand with good accuracy.

The remainder of this paper is organized as follows. Section II provides a brief summary of the nonlinear PWR model. Section III discusses the DNN structure used for the plant identification and formulates the proposed control scheme. The simulation results are given in Section IV before presenting the conclusion in Section V.

## II. Pressurized water reactor

The PWR model adopted in this study can be found in the literature [25]. The PWR plant model consists of various subsystems, such as the reactor core, thermal hydraulics, steam generator, piping and plenum, pressurizer, and turbine-governor system. For a detailed and complete description of the entire NPP model, the readers are kindly referred to [25].

### A. Reactor Core Model

The reactor model can be described using the point kinetics equation, with six groups of delayed neutrons precursors' concentration coupled with thermal hydraulics. The model of the reactor core is represented as follows:

$$\frac{dP_n}{dt} = \frac{\rho_t - \sum_{i=1}^{6} \beta_i}{\Lambda} P_n + \sum_{i=1}^{6} \lambda_i C_{in}, \tag{1}$$

$$\frac{dC_{in}}{dt} = \lambda_i (P_n - C_{in}), \qquad i = 1, 2, \dots 6, \tag{2}$$

$$\frac{dT_f}{dt} = H_f P_n - \frac{1}{\tau_f} (T_f - T_{c1}), \tag{3}$$

$$\frac{dT_{c1}}{dt} = H_c P_n + \frac{1}{\tau_c} (T_f - T_{c1}) - \frac{2}{\tau_r} (T_{c1} - T_{cin}), \tag{4}$$

$$\frac{dT_{c2}}{dt} = H_c P_n + \frac{1}{\tau_c} (T_f - T_{c1}) - \frac{2}{\tau_r} (T_{c2} - T_{c1}), \tag{5}$$

$$\rho_{ttl} = \rho_{rd} + \alpha_f T_f + \alpha_c (T_{c1} + T_{c2}), \tag{6}$$

$$\frac{d\rho_{rd}}{dt} = G v_{rd}. \tag{7}$$

In the above equations, $P_n$ is the normalized neutronic power; $C_{in}$ is the normalized delayed neutron precursors' concentration; $\beta_i$ and $\lambda$ are the fraction of delayed neutrons and decay constant, respectively; $\Lambda$ is the prompt neutron lifetime; $\rho_{ttl}$ and $\rho_{rd}$ represent the total reactivity and the reactivity due to the control rod, repectively; $T_f$, $T_{c1}$, and $T_{c2}$ are the temperatures at fuel, coolant node 1 and node 2, respectively. $H_f$ and $H_c$ are proportionality constants; $\tau_c$, and $\tau_r$ are time constants; $\alpha_f$ and $\alpha_c$ denote the temperature coefficients of reactivity due to fuel and coolant, respectively; $G$ and $v_{rd}$ represent the reactivity worth and the rod speed, respectively.

## III. Controller implementation

### A. Proposed Control Approach

Fig. 1 depicts the proposed control architecture (FBL-DNN) for the PWR process. First, offline training is performed for the DNN to learn the dynamics of the nonlinear process. The quasi-Newton algorithm is employed for the training exercise. Based on the DNN model, the FBL technique is applied to the nonlinear plant to create a linear relationship between the virtual control output $v$ and the system output $y$. The last step consists of using a conventional linear PID controller to control the feedback linearized plant.

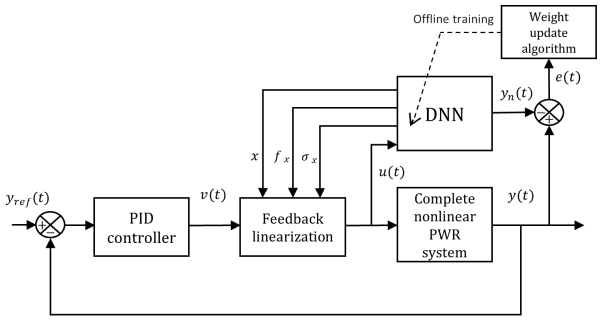


Fig. 1: Block diagram of the proposed control scheme.

#### 1) System Identification Using DNN

System identification is an approach that consists of building mathematical models based on the measurements of the input and output signals of the process [26]. As far as this study is concerned, the system identification is based on DNN for the identification of each subsystem of the PWR system. In contrast to static NNs, which have limited performance in modeling and mapping, DNNs have the capacity to learn complex nonlinear systems. The dynamic neuron model consists of internal dynamics that are added to a static neuron and consist of making the activity of the neuron dependent on its internal state. The DNN of interest is formed by a single layer and described in [23], [26]. The DNN can be represented by the following vector equation:

$$\dot{x}_n = -\beta_n x_n + \omega_n \sigma(x_n) + \gamma_n u_n \tag{8}$$

$$\hat{y}_n = C_n x_n \tag{9}$$

where $x_n$, $y_n$, and $u_n$ are the vector state, the estimated vector output, and the vector input of the DNN, respectively; $\beta_n$, $\omega_n$, and $\gamma_n$ are the adjustable weights; and $\sigma(x_n)$ is the activation function. An identification procedure using a DNN is based on a comparison between the process output and the computed output of the DNN. The goal is to adjust the weights of the DNN to identically reflect the behaviour of the real plant. To accomplish this, a quadratic error function is defined and minimized using the quasi-Newton algorithm. This technique is used for each subsystem of the plant. For brevity, only the reactor is considered here. To identify the reactor, data from the rod speed ($v_{rd}$) and the reactor power ($P_n$) are collected for training the DNN. In total, 3,000 data points are collected and split into two sets of equal length for training and validation. For training purposes, the data are scaled to the range of [-1;1]. The best model obtained is a second order. The trajectories of the estimated output ($x_1$) are shown in Fig. 2, and the DNN model obtained for the

reactor (DNN$_r$) is represented by the state-space model in (10). The DNNs obtained for the other subsystems are also second order.

$$\begin{cases} \dot{x} = f(x) + g(x)\,u \\ y = \quad h(x) = x_1 \end{cases} \tag{10}$$

with $f(x)$ representing the system function, and $g(x)$ the input mapping,

$$f(x) = -\underbrace{\begin{bmatrix} \beta_1 & 0 \\ 0 & \beta_2 \end{bmatrix}}_{\beta_r} \begin{bmatrix} x_1 \\ x_2 \end{bmatrix} + \underbrace{\begin{bmatrix} \omega_{11} & \omega_{12} \\ \omega_{21} & \omega_{22} \end{bmatrix}}_{\omega_r} \begin{bmatrix} \sigma(x_1) \\ \sigma(x_2) \end{bmatrix} \tag{11}$$

$$g(x) = \underbrace{\begin{bmatrix} \gamma_1 \\ \gamma_2 \end{bmatrix}}_{\gamma_r} \tag{12}$$

where $x_1$ and $x_2$ are the output and hidden states of DNN$_r$, respectively. $\beta_r$, $\omega_r$, and $\gamma_r$ are adjustable with respect to DNN$_r$. Their values are:

$$\begin{aligned} &\beta_r = \begin{bmatrix} 0.051 & 0 \\ 0 & 0.102 \end{bmatrix}; \omega_r = \begin{bmatrix} 0.452 & 0.053 \\ -0.14 & 0.053 \end{bmatrix}; \\ &\gamma_r = \begin{bmatrix} 0.115 & -0.073 \end{bmatrix}^T; \end{aligned} \tag{13}$$

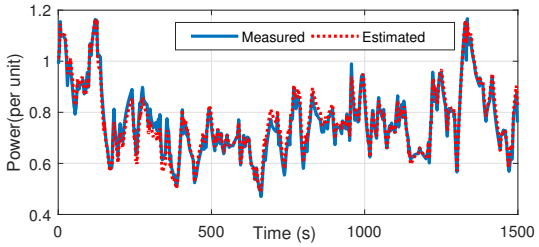


(a) Reactor power training trajectories.

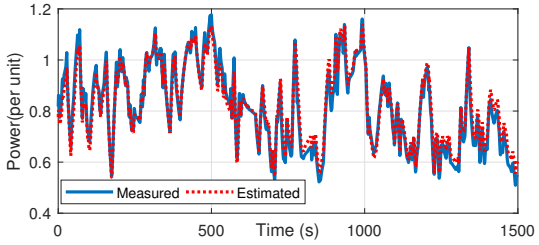


(b) Reactor power validation trajectories.

Fig. 2: Measured and estimated reactor power signals

*2) Input-Output Feedback Linearization*

Based on the state-space model (10), the relative degree $r$ is found to be 1 because the control input appears in the first derivative of $y$

$$\begin{aligned} y &= h(x) = x_1, \qquad (14) \\ \dot{y} &= L_f h(x) + L_g h(x)\,u, \\ &= -\beta_1 x_1 + \omega_{11}\sigma(x_1) + \omega_{12}\sigma(x_2) + \gamma_1 u. \qquad (15) \end{aligned}$$

In the above equations, $L_f h(x)$ stands for the Lie derivative of $h(x)$ with respect to $f(x)$

$$L_f h(x) = \frac{\partial h(x)}{\partial x} f(x) \tag{16}$$

and, likewise, the Lie derivative of $h(x)$ with respect to $g(x)$

$$L_g h(x) = \frac{\partial h(x)}{\partial x} g(x) \tag{17}$$

Considering $r$ = 1, the system can be linearized by the following control law [23]:

$$\begin{aligned} u &= \frac{v - \sum_{k=0}^{r} \lambda_k L_f^k h(x)}{\lambda_r L_g L_f^{r-1} h(x)} \\ &= \frac{v - \lambda_0 x_1 + \lambda_1(\beta_1 x_1 - \omega_{11}\sigma(x_1) - \omega_{12}\sigma(x_2))}{\lambda_1 \gamma_1} \end{aligned} \tag{18}$$

where $v$ is the new input and $\hat{\lambda}_k$ are arbitrary values. Finally, a carefully tuned linear PID controller is added to improve system performance.

## IV. Simulation Results

Simulations are performed to assess the designed controller (FBL-DNN) on a nonlinear PWR plant. The plant is assumed to be initially operating at a steady state. The proposed controller is applied to each of the five control loops of the system: the reactor, steam generator, pressurizer pressure and level, and turbine loop. Here, external disturbances are considered and applied to the control signal of each loop. This disturbance signal can be expressed as follows [9]:

$$\zeta(t) = \zeta_0 sin(10^{-1} t) \tag{19}$$

where $\zeta_0$ is the signal amplitude. The performance of the FBL-DNN controller is compared with that of the classical subspace model predictive control (SPC) strategy. Also, two numerical measures are computed to analyze the control performance: The percentage root mean square error (PRMSE) analyzes the tracking performance, and the L2-norm ($L_2$n) is used to analyze the control effort. These are expressed as follows:

$$\text{PRMSE} = \sqrt{\frac{1}{N}\sum_{i=1}^{N}(y_i - r_i)^2} \times 100\% \tag{20}$$

$$L_2 n = \sqrt{\sum_{i=1}^{N}(u_i)^2} \tag{21}$$

### A. Reactor Power Control Loop

The reactor power control loop is tested in the load-following mode of operation in the presence of the disturbance $\zeta(t)$, with a magnitude $\zeta_0 = 10^{-1}$ that is injected into the rod speed. The performance of the controllers for the reactor loop is shown in Fig. 3, and the reactor power variation is shown in Fig. 3a. The power demand level

imposed is described as follows: the plant is initially assumed to be at full power. The demand is maintained at full power for 200 s, then brought down to 0.8 fractional full power (FFP) in 100 s, maintained at 0.8 FFP for 300 s, and finally, it is brought back to its initial value. It can be seen that FBL-DNN tracks the reference smoothly and accurately despite the disturbance. The classic SPC is also able to follow the desired reference; however, it presents sustained oscillations around the set-point. The control rod speed and reactivity variations are displayed in Fig. 3b and 3c, respectively. The effect of the disturbances can also be seen on the control rod speed for the SPC controller. FBL-DNN deals with the disturbances better than the classical SPC. Table I presents the values of PRMSE and $L_2$n measures that are computed to evaluate the performance of the controllers. It can be seen that the PRMSE value of FBL-DNN is lower than that of the SPC controller. The PRMSE of FBL-DNN is, indeed, half an order of magnitude lower than the classical SPC. Both controllers exert more or less similar control efforts with respect to $L_2$n.

### *B. Steam Generator Control Loop*

In this study, performance of the proposed controller is tested for a reference change in the steam pressure in the presence of the disturbance $\zeta(t)$ with a magnitude $\zeta_0 = 10^{-1}$. The latter is injected into the control input. The steam pressure demand is initially at 7.3 MPa. It is changed to 7.33 MPa in 100 s, maintained at 7.33 MPa for 200 s, then it returns to its initial value. Fig. 4 depicts the performance of the two controllers, and Fig. 4a shows the steam pressure variation. It can be seen that FBL-DNN tracks the set-point with good accuracy, whereas sustained oscillations can be seen for the classical SPC. The control signal response is shown in Fig. 4b. It is clear that the classical SPC spends more control energy than FBL-DNN. In Table I, it can be noticed that FBL-DNN has better tracking accuracy with minimum PRMSE. The $L_2$n value also shows that the FBL-DNN controller exerts less control effort than that of the classical SPC.

### *C. Pressurizer Control Loop*

#### *1) Pressurizer Pressure Loop*

The pressurizer pressure is regulated by controlling a bank of heaters. The controllers are evaluated for a reference change in the pressurizer pressure under disturbances. The disturbance $\zeta(t)$ with an amplitude of $\zeta_0$ = 10 is injected into the heater input. The pressure demand is initally at 15.41 Mpa. In 200 s, it is changed to 15.46 Mpa and maintained there. The performance of the controllers is shown in Fig. 5, and the variation of the pressurizer pressure is displayed in Fig. 5a. It can be seen that both controllers are able to follow the reference trajectory, but it is noticeable that the classical SPC is affected by the disturbances. In fact, it presents an overshoot ratio of 2% that is followed by sustained oscillations around the set-point. The control signal variation is shown in Fig. 5b. The disturbances can be clearly seen in the control input for the classical SPC, whereas FBL-DNN

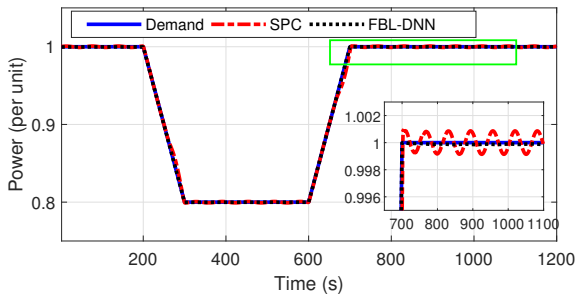


(a) Reactor power.

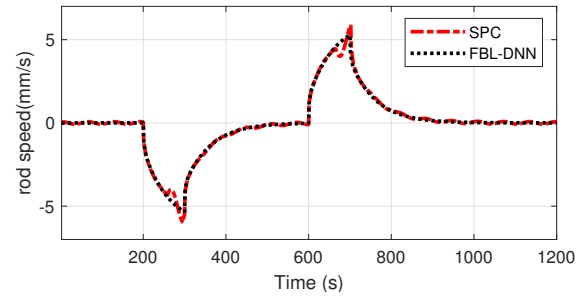


(b) Control rod speed.

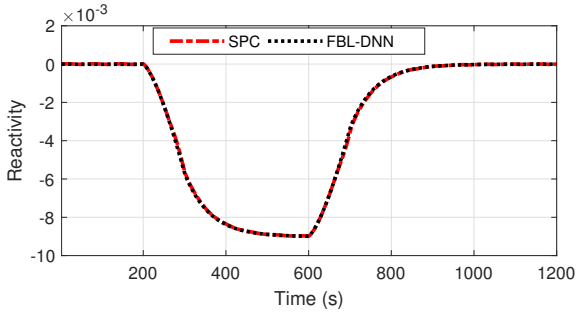


(c) Reactivity.

Fig. 3: Evolution of reactor power signals during the load-following mode.

is able to achieve smooth control. Table I shows that the PRMSE is lower for FBL-DNN than for the classical SPC. The PRMSE of FBL-DNN is three orders of magnitude lower than that of the classical SPC. $L_2$n values also show that the classical SPC exerts slightly less control effort than the proposed strategy but fails at dealing with the disturbances.

#### *2) Pressurizer Level Control Loop*

The control of the pressurizer level aims to maintain the water level of the reactor coolant. The performance of the controllers is evaluated for a reference change in the pressurizer level under the disturbance $\zeta(t)$ with an amplitude of $\zeta_0$ = 10. The performance of the pressurizer level controller is shown in Fig. 6, with the level and control signal responses shown in Fig. 6a and Fig. 6b, respectively. It can be seen that the classical SPC is not able to reject the disturbances as it follows the set-point with an overshoot of 0.6% and is followed by hunting. Conversely, the FBL-DNN controller has good reference tracking and is able of handle the disturbances. From Table I, it is clear that FBL-DNN performs better, given that its PRMSE is four orders

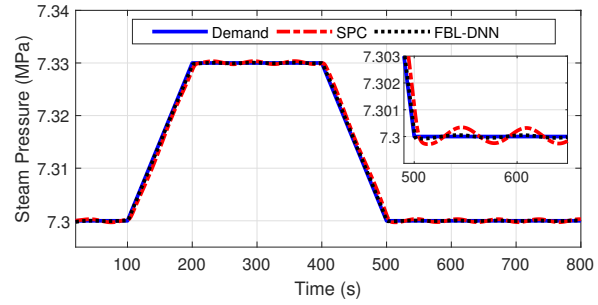


(a) Steam generator secondary pressure.

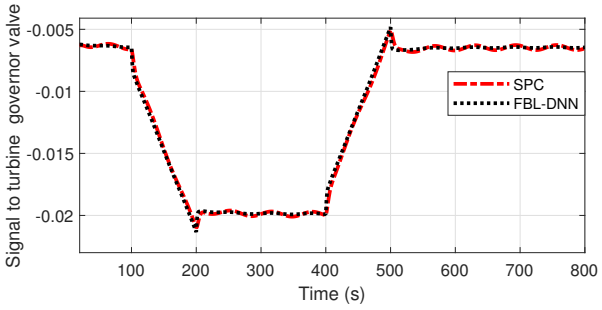


(b) Control signal to turbine govervor valve.

Fig. 4: Evolution of steam generator signals for a set-point change in secondary pressure

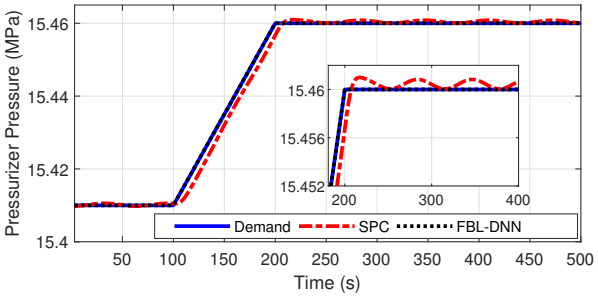


(a) Pressurizer pressure.

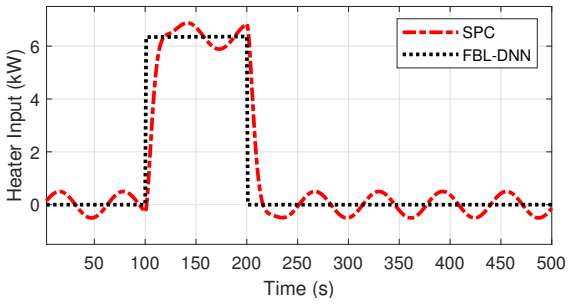


(b) Rate of heat addition.

Fig. 5: Evolution of pressurizer heater signals for a set-point change in pressure

of magnitude lower than the classical SPC. FBL-DNN is also found to exert less control effort in terms of $L_2$n. The proposed controller performs better with minimum control effort.

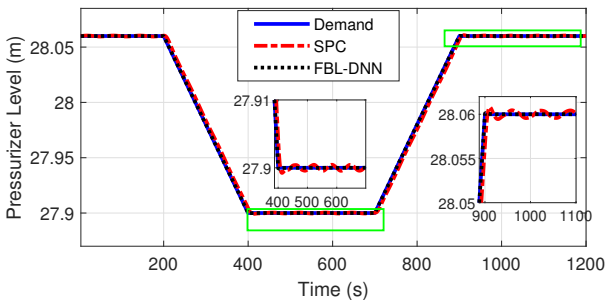


(a) Pressurizer level.

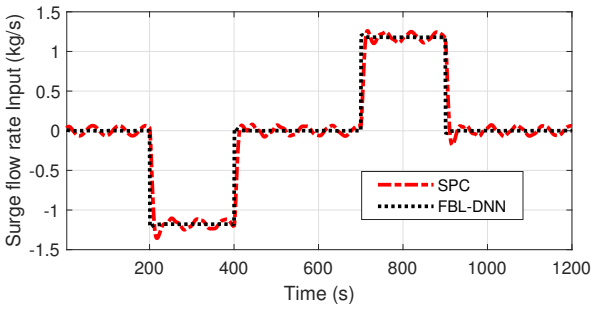


(b) Control signal to CVCS system.

Fig. 6: Evolution of pressurizer level signals for a set-point change in level

TABLE I: Comparison of the Control Techniques

| Case | Technique | PRMSE | $L_2$n |
|---|---|---|---|
| Reactor | SPC | $1.562 \times 10^{-1}$ | $6.430 \times 10^{1}$ |
| | FBL-DNN | $1.304 \times 10^{-2}$ | $6.460 \times 10^{1}$ |
| Steam generator | SPC | $1.086 \times 10^{-3}$ | $9.070 \times 10^{-3}$ |
| | FBL-DNN | $8.800 \times 10^{-4}$ | $8.970 \times 10^{-3}$ |
| Pressurizer pressure | SPC | $2.075 \times 10^{-1}$ | $6.330 \times 10^{4}$ |
| | FBL-DNN | $3.070 \times 10^{-4}$ | $6.350 \times 10^{4}$ |
| Pressurizer level | SPC | $2.522 \times 10^{-1}$ | $2.360 \times 10^{1}$ |
| | FBL-DNN | $1.890 \times 10^{-5}$ | $2.355 \times 10^{1}$ |
| Turbine | SPC | $1.920 \times 10^{-2}$ | $1.180 \times 10^{1}$ |
| | FBL-DNN | $4.498 \times 10^{-3}$ | $1.190 \times 10^{1}$ |

### *D. Turbine Control Loop*

The performance of the control technique is tested for a reference change in the turbine output under the disturbance $\zeta(t)$ with an amplitude $\zeta_0 = 10^{-3}$. Fig. 7 shows the performance obtained for the turbine control loop and Fig. 7 the variation of the turbine output. Both controllers are able to track the set-point, however, the classical SPC has a settling time of 378 s and settles with residual oscillations. The control signal variation is shown in Fig.7b. The two control strategies exert nearly the same control effort in terms of $L_2$n. The PRMSE value verifies the better accuracy of the proposed controller over the classical SPC. Overall, the two controllers produce similar control effort, but FBL-DNN offers better robustness and accuracy.

## V. Conclusion

A DNN-based FBL strategy is designed to control an entire PWR. The nonlinear plant is linearized using the

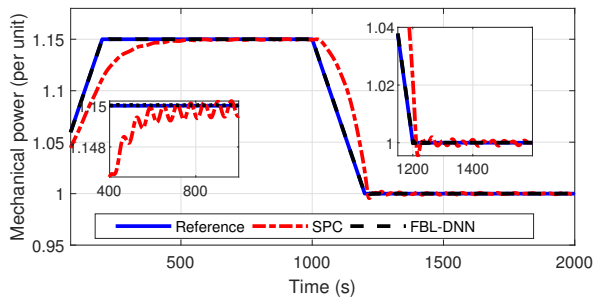


(a) Mechanical power.

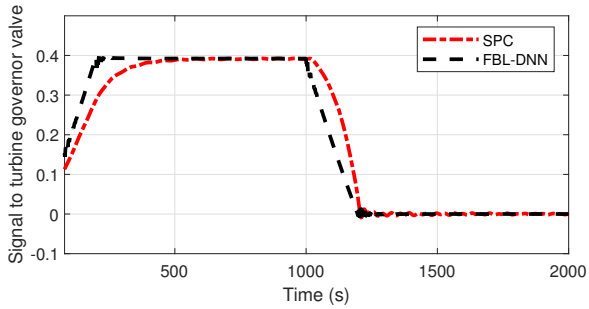


(b) Control signal to turbine govervor valve.

Fig. 7: Evolution of the turbine-speed signals for a set-point change in demand power of the generator.

offline trained DNN and the FBL technique. A PID controller is then applied to the linearized system to improve the performance of the PWR plant. The proposed strategy has been tested on the different loops of the PWR. Control strategies for the reactor power, steam pressure, pressurizer pressure and level, and turbine speed have been implemented and validated. The simulation results verify that the proposed controller offers good performance and improved robustness under disturbances. The proposed technique is found to perform better than the classical SPC controller.

## VI. Acknowledgment

This work was financially supported by the Engineering and Physical Sciences Research Council (grant: EP/R021961/1).

## References

[1] Y. Oka, K. Suzuki *et al.*, *Nuclear Reactor Kinetics and Plant Control*. Springer, 2013, vol. 10.

[2] C. Liu, J.-F. Peng, F.-Y. Zhao, and C. Li, "Design and optimization of fuzzy-pid controller for the nuclear reactor power control," *Nuclear Engineering and Design*, vol. 239, no. 11, pp. 2311–2316, 2009.

[3] Z. Dong, "Pd power-level control design for pwrs: A physically-based approach," *IEEE Transactions on Nuclear Science*, vol. 60, no. 5, pp. 3889–3898, 2013.

[4] S. M. H. Mousakazemi, N. Ayoobian, and G. R. Ansarifar, "Control of the pressurized water nuclear reactors power using optimized proportional–integral–derivative controller with particle swarm optimization algorithm," *Nuclear Engineering and Technology*, vol. 50, no. 6, pp. 877–885, 2018.

[5] S. M. H. Mousakazemi, "Control of a pwr nuclear reactor core power using scheduled pid controller with ga, based on two-point kinetics model and adaptive disturbance rejection system," *Annals of Nuclear Energy*, vol. 129, pp. 487–502, 2019.

[6] R. Banavar and U. Deshpande, "Robust controller design for a nuclear power plant using h/sub/spl infin//optimization," *IEEE Transactions on nuclear science*, vol. 45, no. 2, pp. 129–140, 1998.

[7] X. Yan, P. Wang, J. Qing, S. Wu, and F. Zhao, "Robust power control design for a small pressurized water reactor using an h infinity mixed sensitivity method," *Nuclear Engineering and Technology*, vol. 52, no. 7, pp. 1443–1451, 2020.

[8] G. Li, "Modeling and lqg/ltr control for power and axial power difference of load-follow pwr core," *Annals of Nuclear Energy*, vol. 68, pp. 193–203, 2014.

[9] V. Vajpayee, V. M. Becerra, N. Bausch, J. Deng, S. R. Shimjith, and A. J. Arul, "Lqgi/ltr based robust control technique for a pressurized water nuclear power plant," *Annals of Nuclear Energy*, vol. 154, p. 108105, 2021.

[10] L. Wei, F. Fang, and Y. Shi, "Adaptive backstepping-based composite nonlinear feedback water level control for the nuclear u-tube steam generator," *IEEE Transactions on Control Systems Technology*, vol. 22, no. 1, pp. 369–377, 2014.

[11] Z. Dong, J. Feng, X. Huang, and L. Zhang, "Power-level control of nuclear reactors based on feedback dissipation and backstepping," *IEEE Transactions on Nuclear Science*, vol. 57, no. 3, pp. 1577–1588, 2010.

[12] G. R. Ansarifar and S. Saadatzi, "Nonlinear control for core power of pressurized water nuclear reactors using constant axial offset strategy," *Nuclear Engineering and Technology*, vol. 47, pp. 838–848, 2015.

[13] M. Zaidabadi nejad and G. Ansarifar, "Robust feedback-linearization control for axial power distribution in pressurized water reactors during load-following operation," *Nuclear Engineering and Technology*, vol. 50, no. 1, pp. 97–106, 2018.

[14] Y. Liu, J. Liu, and S. Zhou, "Linear active disturbance rejection control for pressurized water reactor power based on partial feedback linearization," *Annals of Nuclear Energy*, vol. 137, p. 107088, 2020.

[15] J. de Jesús Rubio, P. Angelov, and J. Pacheco, "Uniformly stable backpropagation algorithm to train a feedforward neural network," *IEEE Transactions on Neural Networks*, vol. 22, no. 3, pp. 356–366, 2011.

[16] M. N. Khajavi, M. B. Menhaj, and A. A. Suratgar, "A neural network controller for load following operation of nuclear reactors," *Annals of Nuclear Energy*, vol. 29, no. 6, pp. 751–760, 2002. [Online]. Available: https://www.sciencedirect.com/science/article/pii/S0306454901000755

[17] H. Arab-Alibeik and S. Setayeshi, "Adaptive control of a pwr core power using neural networks," *Annals of Nuclear Energy*, vol. 32, no. 6, pp. 588–605, 2005.

[18] Z. Dong, "A neural-network-based nonlinear adaptive state-observer for pressurized water reactors," *Energies*, vol. 6, no. 10, pp. 5382–5401, 2013.

[19] R. Coban, "A context layered locally recurrent neural network for dynamic system identification," *Engineering Applications of Artificial Intelligence*, vol. 26, no. 1, pp. 241–250, 2013.

[20] J. Deng, "Dynamic neural networks with hybrid structures for nonlinear system identification," *Engineering Applications of Artificial Intelligence*, vol. 26, no. 1, pp. 281–292, 2013.

[21] J. Deng, V. Becerra, and R. Stobart, "Input constraints handling in an mpc/feedback linearization scheme," *International Journal of Applied Mathematics and Computer Science*, vol. 19, no. 2, p. 219, 2009.

[22] J. O. Pedro, M. Dangor, O. A. Dahunsi, and M. M. Ali, "Dynamic neural network-based feedback linearization control of full-car suspensions using pso," *Applied Soft Computing*, vol. 70, pp. 723–736, 2018.

[23] A. Naimi, J. Deng, S. R. Shimjith, and A. J. Arul, "Dynamic neural network-based feedback linearization control of a pressurized water reactor," in *2020 13th International Conference on Developments in eSystems Engineering (DeSE)*, 2020, pp. 228–232.

[24] A. Naimi, J. Deng, V. Vajpayee, V. Becerra, S. Shimjith, and A. J. Arul, "Nonlinear model predictive control using feedback linearization for a pressurized water nuclear power plant," *IEEE Access*, vol. 10, pp. 16 544–16 555, 2022.

[25] V. Vajpayee, V. Becerra, N. Bausch, J. Deng, S. Shimjith, and A. J. Arul, "Robust-optimal integrated control design technique for a pressurized water-type nuclear power plant," *Progress in Nuclear Energy*, p. 103575, 2020.

[26] F. R. Garces, V. M. Becerra, C. Kambhampati, and K. Warwick, *Strategies for feedback linearisation: a dynamic neural network approach*. Springer Science & Business Media, 2002.